
Chapter 4. Time domain characterisation of antennas by normalised impulse response

4.1. Introduction

When antennas are excited with a simple harmonic, the frequency dependency of the antenna parameters is usually investigated in the frequency domain over the frequency band of interest. In time domain systems like time domain GPRs, antennas are excited by a fast transient pulse. When using antennas to radiate fast transient pulses, referred to as *time domain antennas*, classical antenna parameters such as gain, radiation pattern, and phase centre, have less meaning [1]. All these parameters are frequency dependent, hence they have to be expressed over the whole frequency band of interest. As time domain antennas have intrinsically a large bandwidth, describing the antenna performances with the frequency dependent parameters is not convenient and most of all not compact. On the other hand, other parameters become more important for time domain antennas, such as ringing in the antenna, maximum amplitude of the received signal, duration of a response, etc. These are all important parameters for an ultra-wideband radar system, where the performance often depends on the quality of the raw data prior to processing. Furthermore, there is a need for describing the antenna performances in a compact way, which can be used for modelling, or for comparing performances of different time domain antennas.

4.2. Definitions of terms

4.2.1. Impulse response and frequency response function

Every time-invariant linear system is completely described in the time domain by its Impulse Response (IR) $h(t)$, which mathematically relates the input $x(t)$ to the output $y(t)$ of the system, by the convolution integral

$$y(t) = \int_{-\infty}^{+\infty} h(\mathbf{t})x(t-\mathbf{t})d\mathbf{t} \quad (4.1)$$

where $x(t)$ is the input signal,

$y(t)$ the output signal,

and $h(t)$ the impulse response of the system (Fig. 4-1).

Equation (4.1) can be written using the convolution operator \otimes :

$$y(t) = h(t) \otimes x(t) \quad (4.2)$$

The IR depends on what one takes as input and output of the system. In the frequency domain the corresponding relation is given by the Fourier transformation of (4.2)

$$Y(j\omega) = H(j\omega)X(j\omega) \quad (4.3)$$

where $X(j\omega)$ and $Y(j\omega)$ are the respective Fourier transforms of the input $x(t)$ and the output $y(t)$. $H(j\omega)$, defined as the *Frequency Response Function*, is the Fourier transform of the impulse response $h(t)$:

$$H(j\omega) = \frac{1}{2\pi} \int_{-\infty}^{+\infty} h(t) e^{-j\omega t} dt \quad (4.4)$$

Related by the Fourier transform, $H(j\omega)$ and $h(t)$ contain the same information.

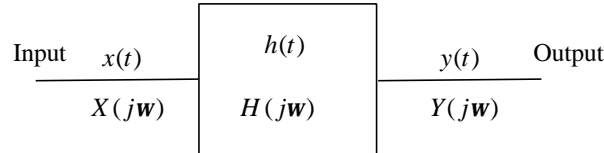


Fig. 4-1: Representation of a time-invariant, stable and linear system

According to equation (4.2), if the system is excited by a Dirac impulse $\mathbf{d}(t)$, the output becomes $h(t)$, hence the name impulse response:

$$\begin{aligned} y(t) &= h(t) \otimes \mathbf{d}(t) \\ &= h(t) \end{aligned}$$

4.2.2. Virtual source of a time domain antenna

In the time domain characterisation of the antennas we will often need the distance from an observation point in the far field to the antenna. Due to the finite but non-zero dimension of the antenna, this distance becomes ambiguous. To solve this, we have defined for our convenience an apparent point in the antenna from which the magnitude of the radiated field $\vec{E}_{rad}(\vec{r}, t)$ degrades with a factor $1/R$ (free space loss or spreading loss) in the far field, where R is the distance from that apparent point. We call this point the "virtual source" of the antenna [2].

The virtual source can be considered as the time equivalent of the phase centre. The phase centre of an antenna is a frequency concept and is defined by IEEE (Std 145-1983) as: "The location of a point associated with an antenna such that, if it is taken as the centre of a sphere whose radius extends into the far field, the phase of a given field component over the surface of the radiation sphere is essentially constant, at

least over that portion of the surface where the radiation is significant.” Equivalent to this definition, we can consider the virtual source to be the origin of a sphere formed by the wave front of the radiated pulse-shaped spherical TEM wave at a certain time.

The virtual source is in general located between the antenna feed and the aperture. In the time domain characterisation of the antennas, the virtual source will serve as origin of the co-ordinate system $\vec{r} = \vec{0}$, unless specified otherwise.

4.2.3. The far field for time domain antennas

The definition of the far field is a good example of how inconvenient it can be to use classical antenna parameters in the time domain. IEEE defines the far field in Std 145-1983 as “The region of the field where the normalised angular field distribution is essentially independent of the distance from a specified point in the antenna region “. In this region the power density also varies as R^{-2} . For a narrow band antenna, the far field distance is taken as the distance R from the antenna phase centre where the phase shift between the ray from the aperture edge and that from the centre is 22.5° . For most narrow band antenna, this distance R corresponds with

$$R = \frac{2D^2}{\lambda} \quad (4.5)$$

where D is the aperture dimension in meters and λ the wavelength in free space.

This would mean that for ultra-wideband antennas the far field distance is a function of frequency. In [1] E. G. Farr and C. E. Baum propose an extension of the far field definition into the time domain. To be in the far field of a time domain antenna, the clear time between the arrival of the closest ray and the arrival of the outermost ray should be small compared with the full-width-half-maximum (FWHM) of the pulse (or 10-90% risetime in case of a step). This means

$$\frac{(d_2 - d_1)}{c} \leq \frac{t_{FWHM}}{\mathbf{n}} \quad (4.6)$$

with d_1 and d_2 as defined in Fig. 4-2, and \mathbf{n} a constant that identifies how much larger the FWHM is than the clear time. The question is how large should \mathbf{n} be taken? The authors suggest \mathbf{n} in the region of three to five.

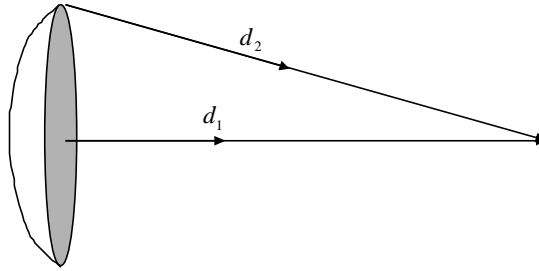


Fig. 4-2: Configuration for far field calculation

In this work we will use another definition for the far field of a time domain antenna, more similar to the R^{-2} dependency of the radiated power in the far field of narrow band antennas. We consider to be in the far field of the time domain antenna if the peak value of the radiated field component varies as R^{-1} , with R the distance from the virtual source. In this definition, just like in the definition of E. G. Farr and C. E. Baum, the far field distance will be function of the transient pulse shape.

4.2.4. Electrical boresight

The electrical boresight of a highly directive antenna is the direction at which the largest signal appears. For time domain antennas this definition holds. A TEM horn antenna normally radiates the maximum amplitude in the symmetry axis of the horn. As for the dielectric-filled TEM horn, developed in Chapter 2, the structure is not totally symmetrical due to the integrated balun, the electrical boresight will be slightly different from the symmetry axis. For simplicity however, we consider the electrical boresight in the symmetry axis of the antenna.

4.2.5. Definition of patterns for time domain antennas

The antenna pattern or radiation pattern is defined by IEEE as: “The spatial distribution of a quantity which characterises the electromagnetic field generated by an antenna”. The quantity, which is most often used to characterise the radiation is the directivity. In this case the antenna pattern $k(\mathbf{q}, \mathbf{j})$ can be written as

$$k = D(\mathbf{q}, \mathbf{j}) / D_M \quad (4.7)$$

where

$D(\mathbf{q}, \mathbf{j})$ is the directivity of the antenna, defined as the ratio of the active power density radiated by the antenna in a given direction to the active power density that would be radiated in the same direction by an isotropic antenna, radiating the same power as the antenna of interest,

D_M is the maximal directivity.

For an UWB antenna this pattern will change as a function of frequency. The antenna will be less directive for lower frequencies and more directive for higher frequencies.

If antennas are used to radiate fast transient pulses, the following quantities seem more useful [3]:

1. The peak power received in a pulse. It does not contain however any information on the change in pulse shape
2. The peak value when the off-axis pulse is correlated with the on-boresight pulse
3. The power in the pulse, integrated over the length of the pulse
4. The peak-to-peak value of the received pulse.

Each quantity has its advantages, depending on the application. In our application, the most convenient quantity seemed to be the last one. We will refer to it as the p-t-p

antenna pattern, and the quantity which characterises the field is the peak-to-peak value of the received pulse normalised to the peak-to-peak value of the received pulse on boresight.

4.3. Time domain antenna equations

A common way of describing systems in the time domain is by means of an impulse response (IR). An antenna can be considered as a linear time-invariant system. For a given defined input and output, the antenna is totally characterised by its IR, relating the input to the output with the convolution integral. This relationship is referred to as an antenna equation in the time domain.

In this section, the antenna equations are expressed first in terms of conventional IR, and later (Section 4.4) in terms of normalised IR. To simplify the expressions, we only consider antenna performance for dominant linear polarisation of the E-field. The extension to the more general case is possible without too much effort. Furthermore we consider the input and output impedance of the laboratory equipment like voltage source, sampling oscilloscope, vector network analyser and cables used, matched to $50\ \Omega$ (denoted Z_c). We define V_s as the voltage generated by the source in a $50\ \Omega$ load and V_{rec} as the voltage measured by an oscilloscope with a $50\ \Omega$ input impedance (see Fig. 4-3). We also consider that we have two identical antennas.

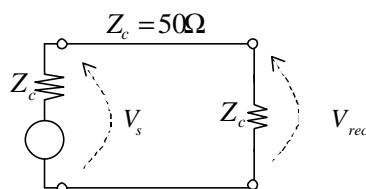


Fig. 4-3: Definition of symbols

4.3.1. Transmitting antenna

First consider the case of the transmitting antenna, near the co-ordinate origin $\vec{r} = \vec{0}$. As input we consider a voltage V_s applied at the input reference plane (Fig. 4-4).

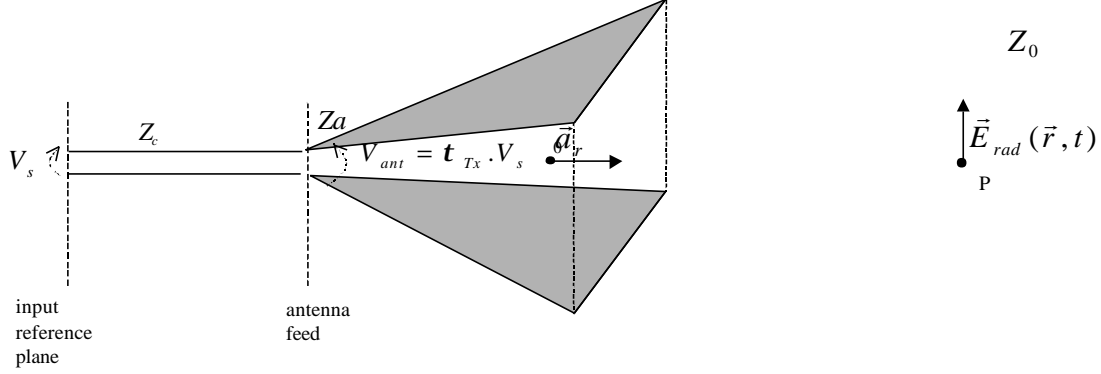


Fig. 4-4: Transmitting antenna configuration

The radiated field $\vec{E}_{rad}(\vec{r}, t)$ in a point P in the far field, for $\vec{r} \rightarrow \infty$, can be described as [2] [4] [5]

$$\vec{E}_{rad}(\vec{r}, t) = \frac{1}{2\pi r c f_g} \frac{d\vec{h}_{Tx}(\vec{a}_r, t)}{dt} \otimes V_{ant}(t) \otimes \mathbf{d}(t - t_{d, TX}) \quad (4.8)$$

with $V_{ant} = \mathbf{t}_{Tx} V_s$, $\mathbf{t}_{Tx} = \frac{2Z_a}{Z_c + Z_a}$, $f_g = \frac{Z_a}{Z_0}$

where $h_{TX}(\vec{a}_r, t)$ is defined as the IR of the transmitting antenna in the direction $\vec{a}_r = \frac{\vec{r}}{|\vec{r}|}$, r is defined to be $r = |\vec{r}|$, V_{ant} is the excitation voltage at the antenna feed, \mathbf{t}_{Tx} the voltage transmission coefficient from the feed cable to the antenna, Z_a the antenna input impedance, assumed to be a real constant, and $Z_0 = 120\pi$. The convolution with the Dirac-function $\mathbf{d}(t - t_{d, TX})$ in (4.8) introduces a total delay $t_{d, TX}$, which corresponds to the propagation time between the input of the antenna system

where V_s is applied (input reference plane) and the observation point P where $\vec{E}_{rad}(\vec{r}, t)$ is evaluated.

For uniformity reasons, we use \vec{h}_{Tx} as kernel for the convolution in (4.8) and derive the input signal V_s . In the frequency domain, this corresponds to multiplying the input signal by the complex frequency s and the derivative of the IR by $1/s$. Taking into account the simplification of working only for dominant linear polarisation of the E-field, (4.8) can then be rewritten as

$$E_{rad}(\vec{r}, t) = \frac{t_{Tx}}{2\pi r c f_g} h_{Tx}(\vec{a}_r, t) \otimes \frac{dVs(t)}{dt} \otimes \mathbf{d}(t - t_{d, TX}) \quad (4.9)$$

As discussed in [5], for finite $r = |\vec{r}|$, one should limit the highest frequency for such result to be valid. Recognising these limitations, we introduce another problem. Due to the finite but non-zero dimension of the antenna, the location of the coordinate system origin $\vec{r} = \vec{0}$ becomes ambiguous. To solve this we take the coordinate system origin in the virtual source of the antenna, as defined in Section 4.2.2. When defining the origin of the coordinate system $\vec{r} = \vec{0}$ in this point, equation (4.9) is valid for finite $r = |\vec{r}|$. Assuming that the position of the virtual source is frequency independent over the frequency band of interest (this has been verified experimentally for a dielectric filled TEM horn), it can easily be located (see Section 4.4.2).

A disadvantage of using expression (4.9) is that Z_a is a function of frequency, so t_{Tx} and f_g are not constant. It will be shown that this difficulty can be eliminated by introducing a normalised IR.

4.3.2. Receiving antenna

Consider now the case of the receiving antenna, with a uniform plane-wave incident E-field $\vec{E}_{inc,VS}(t)$, evaluated in the virtual source point of the receiving antenna (Fig. 4-5). The incident direction is characterised by the unit vector \vec{a}_r .

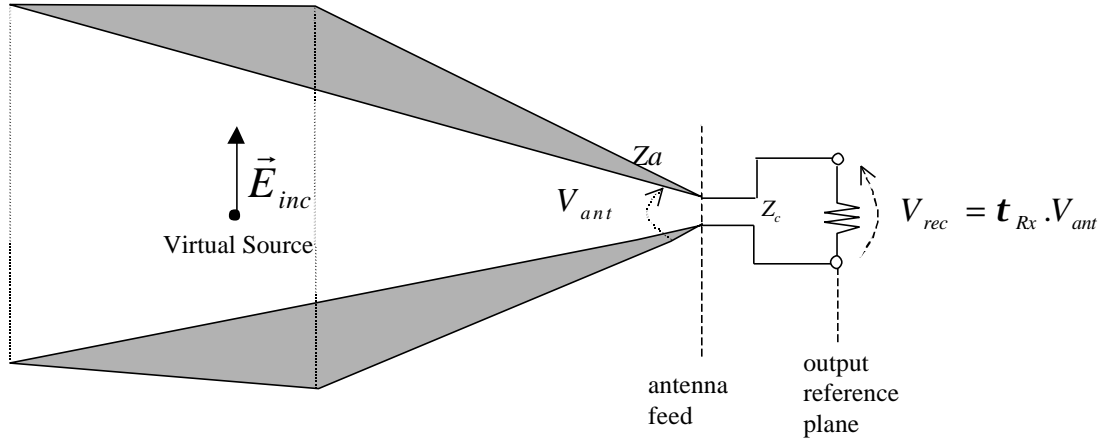


Fig. 4-5: Receiving antenna configuration

For dominant polarisation, the output voltage $V_{rec}(t)$ measured by an oscilloscope in the output reference plane is related to the incident field by [2] [4] [5]

$$V_{rec}(t) = \mathbf{t}_{Rx} h_{Rx}(-\vec{a}_r, t) \otimes E_{inc,VS}(t) \otimes \mathbf{d}(t - t_{d,RX}) \quad (4.10)$$

$$\text{with } \mathbf{t}_{Rx} = \frac{2Z_c}{Z_c + Z_a}$$

where $h_{Rx}(-\vec{a}_r, t)$ is the impulse response of the receiving antenna in the direction $-\vec{a}_r$, and $t_{d,RX}$ represents the total propagation time between the virtual source point of the receiving antenna and the output reference plane where $V_{rec}(t)$ is measured.

Expressions (4.9) and (4.10) are defined such that, if the transmitting and receiving antennas are the same, $h_{Rx} = h_{Tx}$.

4.3.3. Reciprocity of time domain antennas

Let us go for a moment back to the frequency domain. If the same antenna is used to transmit and receive, the frequency response function of the transmitting antenna will not be the same as the frequency response function of the receiving antennas. This can be derived from the Rayleigh-Carson reciprocity theorem [6]. The antenna power gain G_t , which is a transmission characteristic, and the antenna effective area A_e , which is a receiving characteristic, are related by

$$G_t = \frac{4p}{I^2} A_e \quad (4.11)$$

Equation (4.11) is a direct consequence of the Rayleigh-Carson reciprocity theorem.

The far field power density S in [W/m²] at a distance R from the transmitting antenna is given by

$$S = \frac{1}{4pR^2} G_t P_t \quad (4.12)$$

with P_t the excitation power at the antenna feed. Taking the square root of equation (4.12) and recasting into voltages, yields a relation between the radiated electrical field and the excitation voltage. Hence the frequency response function is proportional to $\sqrt{G_t(\omega)}$. On the other hand, when the antenna is used as receiving antenna, the received power as a function of the incoming power density S_{inc} is given by

$$P_r = A_e S_{inc} \quad (4.13)$$

So the frequency response characteristic, relating the incoming field E_{inc} to the received voltage at the antenna feed is proportional to $\sqrt{A_e(\mathbf{w})}$. Hence, according to (4.11), the ratio of the transmit frequency response function of an antenna to the receive frequency response function of the same antenna, is proportional to I^{-1} (or to frequency). The above result holds for any antenna [7]. In other words, the IR of the transmitting antenna has to be proportional to the time derivative of the IR of the receiving antenna. This can also be seen by comparing expression (4.8) and (4.10). In Section 4.3.1 we anticipated on this by defining \vec{h}_{Tx} as IR in (4.9) and derive the input signal V_s . Doing so, $h_{Rx} = h_{Tx}$ if the antennas are the same.

4.4. Normalised impulse response

The disadvantage of using expressions (4.9) and (4.10) is that in reality Z_a is a function of frequency, so that t_{Rx} and f_g are not real constants. It would be logical and easier to integrate this frequency dependent term Z_a in the IR, which is in any event unique for each antenna. This can be done by normalising in expressions (4.9) and (4.10) the fields and voltages to the local characteristic impedance [4].

4.4.1. Normalisation of the IR

When normalising in the antenna equations the voltages and electric fields to the local characteristic impedance, expressions (4.9) and (4.10) can be rewritten as

$$\frac{E_{rad}(\vec{r}, t)}{\sqrt{Z_0}} = \frac{1}{2\mathbf{p}rc} h_{N,Tx}(\vec{a}_r, t) \otimes \frac{1}{\sqrt{Z_c}} \frac{dV_s(t)}{dt} \otimes \mathbf{d}(t - t_{d,TX}) \quad (4.14)$$

$$\frac{V_{rec}(t)}{\sqrt{Z_c}} = h_{N,Rx}(-\vec{a}_r, t) \otimes \frac{E_{inc,VS}(t)}{\sqrt{Z_0}} \otimes \mathbf{d}(t - t_{d,RX}) \quad (4.15)$$

where $h_{N,Tx}$ and $h_{N,Rx}$ are the normalised IRs for transmitting and receiving antenna. They are defined as

$$h_{N,Tx} = \sqrt{\frac{Z_c}{Z_a}} \frac{\mathbf{t}_{Tx}}{\sqrt{f_g}} h_{Tx} \quad \text{and} \quad h_{N,Rx} = \sqrt{\frac{Z_a}{Z_c}} \frac{\mathbf{t}_{Rx}}{\sqrt{f_g}} h_{Rx} \quad (4.16)$$

If the transmitting and receiving antenna are the same, then $h_{N,Rx} = h_{N,Tx}$. Combining expressions (4.14) and (4.15), the received voltage, measured with a 50 ohm oscilloscope at the receiving antenna, can be related to the input voltage by

$$V_{rec}(t) = \frac{1}{2pRC} h_{N,Tx}(\vec{a}_r, t) \otimes h_{N,Rx}(-\vec{a}_r, t) \otimes \frac{dV_s(t)}{dt} \otimes \mathbf{d}(t - t_{d,TX} - t_{d,RX}) \quad (4.17)$$

For equation (4.17) the co-ordinate origin is taken in the virtual source of the transmitting antenna, R is defined as the distance between the two virtual sources of the antennas at boresight, and $t_{d,TX} + t_{d,RX}$ represents the total delay in the combined system. This delay is of importance for the measurement of the normalised impulse response.

Expressions (4.14), (4.15) and (4.17) are extremely simple to use. Due to the elimination of the transmission coefficient between the feed cable and the antenna, and due to the elimination of the antenna impedance in the antenna equations, they can be used without any assumption. Knowing the normalised IR of the antennas, one can calculate, as a function of the input signal, the exact radiated E-field at any point P in the far field of the transmitting antenna. One can also calculate the received voltage for an incoming E-field.

4.4.2. Measurement of Normalised IR on boresight

In a first step we will explain how the normalised IR on boresight can be measured. In a second step we show how the normalised IR in any direction can be derived from the normalised IR on boresight and the p-t-p pattern of the antenna.

But before measuring the normalised IR of an antenna, we first have to locate the virtual source of the antenna. This can be done experimentally by using two identical antennas on boresight. The virtual source can be seen as the origin of the radiated impulse, from which the $1/R$ free space loss is initiated. Let d be the distance between the two antenna apertures, which is easy to measure (Fig. 4-6). For different values of d , the measured voltage V_{rec} degrades with $1/R$ in the far field.

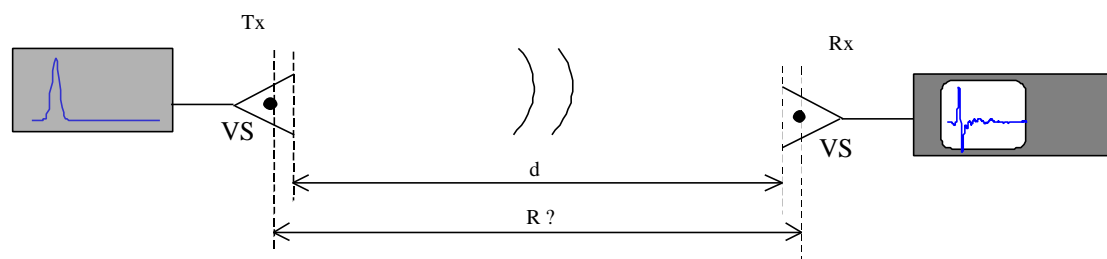


Fig. 4-6: Set-up for locating the virtual source (VS) of an antenna

In Fig 4-7 we present d versus the inverse peak-to-peak value of the received voltage V_{rec} . The zero of the line fitted through these points in the least-squares sense gives the difference between R and d .

In this example $(R - d)$ is 8 cm, so the virtual source is located at 4 cm from the antenna aperture towards the antenna feed. The knowledge of the exact location of the virtual source is important when (4.14), (4.15) or (4.17) are used near the antennas (but still in the far field) or for exact measurement of the normalised IR of an antenna.

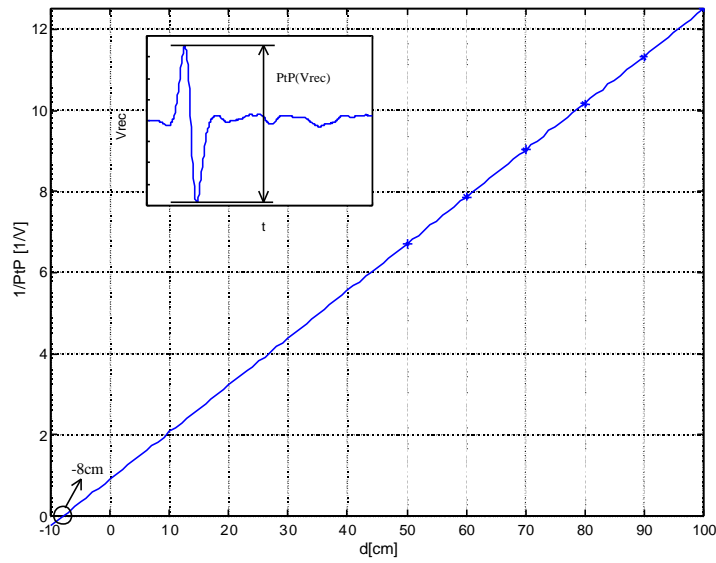


Fig. 4-7: d versus the inverse point to point value of the received voltage V_{rec}

Once the location of the virtual source is known, $h_{N,Tx}$ and $h_{N,Rx}$ can be measured by using two identical antennas and a vector network analyser (VNA). Converting (4.17) into the frequency domain, the normalised frequency response function of the antennas is expressed as

$$H_N(\mathbf{w}) = \sqrt{\frac{2p R c V_{rec}(\mathbf{w})}{j\mathbf{w}V_s(\mathbf{w})}} e^{j\mathbf{w}(t_{d,TX} + t_{d,RX})} \quad (4.18)$$

Considering the two antennas on boresight in the far field, with a distance R between the two virtual sources, as a two-port, one can measure the S_{21} parameter with a VNA over the frequency band of interest, covering at least the whole frequency range of the antenna.

The quantity $t_{d,TX} + t_{d,RX}$, total delay between the reference planes of port 1 and port 2, can be replaced by $\frac{R'}{c}$, where R' is the distance between the two reference planes of the VNA and c the speed of light.

Expression (4.18) can then be written as

$$H_N(\mathbf{w}) = \sqrt{\frac{2\mathbf{p}Rc}{j\mathbf{w}} S_{21}(\mathbf{w}) e^{j\mathbf{w}R/c}} \quad (4.19)$$

In expression (4.19) the square root is taken from a complex number. To do so, one first has to unwrap the phase, otherwise the result is non-physical. The unwrapping is far more easy by taking into account the term $e^{j\mathbf{w}R/c}$, hence its importance.

Once the discrete frequency vector $H_N(\mathbf{w})$ is found, $h_N(t)$ can be extracted by a frequency-time transformation using the following processing scheme:

1. Complete the discrete frequency vector $H_N(\mathbf{w})$ with zeros for missing frequencies between zero and the start frequency of the VNA
2. Pad zeros after the frequency vector to obtain the desired time resolution after frequency-time transformation. The time step after the transformation will be $T_s = 1/(2f_{\max})$, with f_{\max} the highest frequency after zero padding
3. Take the real part of the inverse DFT of the zero-padded frequency vector. Multiply the real part by 2 to obtain the discrete sequence $h_N(n)$ with the desired time step T_s
4. $h_N(t) = h_N(n) / T_s$.

In step 3, the real part of the inverse DFT is multiplied by 2. The factor two takes into account the lag of the negative frequencies in the frequency vector. The same discrete sequence $h_N(n)$ would be found if the frequency vector was first completed for negative frequencies before taking the inverse DFT.

It is not necessary to perform step 4, when using the expression (4.14), (4.15) or (4.17) under its discrete form. The division by T_s in step 4 is explained as follows: when the discrete sequence $x_s(n)$ contains the exact samples of the analogue signal

$x_a(t)$ sampled with a period T_s , the discrete Fourier transform of the discrete signal X_s is then related to the Fourier transform of the analogue signal X_a by [8]

$$X_s(e^{j\omega T}) = \frac{1}{T_s} \sum_{l=-\infty}^{\infty} X_a \left[j \left(\frac{\omega + 2\pi l}{T_s} \right) \right] \quad (4.20)$$

In our case the discrete frequency vector $H_N(\mathbf{w})$ in (4.19) contains the exact samples of its analogue version. So after the inverse DFT, the discrete sequence $h_N(n)$ will be T_s times superior to the exact samples of $h_N(t)$.

4.4.3. Normalised IR off-boresight

In previous section we showed a procedure to measure the normalised IR of the TEM horn on boresight, *i.e.* $\mathbf{q} = 0$ and $\mathbf{j} = 0$ (Fig. 4-8). In this section we will show that this normalised IR on boresight $h_N(\mathbf{q} = 0, \mathbf{j} = 0, t)$ or short $h_{N,0}(t)$, in combination with the antenna pattern, can also be used to describe the behaviour of the TEM horn off-boresight in a given direction (\mathbf{q}, \mathbf{j}) , as far as we stay within the 3dB opening angle of the antenna beam.

The co-ordinate system is shown on Fig 4-8: the origin is defined as usual in the virtual source (VS) of the antenna, \mathbf{j} is the angle in the H-plane of the antenna, and \mathbf{q} the angle in the E-plane, both measured from the boresight direction.

In an experimental study we found that the fast transient impulse radiated by the dielectric TEM horn in a given direction only varies in amplitude, but not in shape along the time axis, as far as we stay within the 3dB beamwidth of the antenna. In other words, the pulse shape along the time axis of the radiated signal in a direction (\mathbf{q}, \mathbf{j}) will be identical to the pulse shape of the signal radiated on boresight. The factor k , representing the variation in amplitude, is by definition given by the p-t-p antenna pattern and can be split in a product of two factors k_h and k_e , representing

the pattern in the H-plane and in the E-plane. To simplify the reasoning, we consider a configuration as shown in Fig. 4-9. The transmitting antenna can only rotate in the H-plane. The receiving antenna stays fixed.

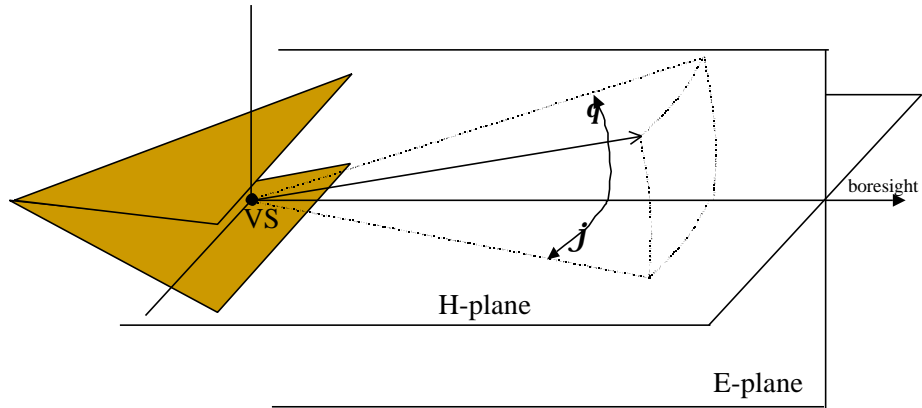


Fig. 4-8: Representation of co-ordinate origin, \mathbf{q} and \mathbf{j} .

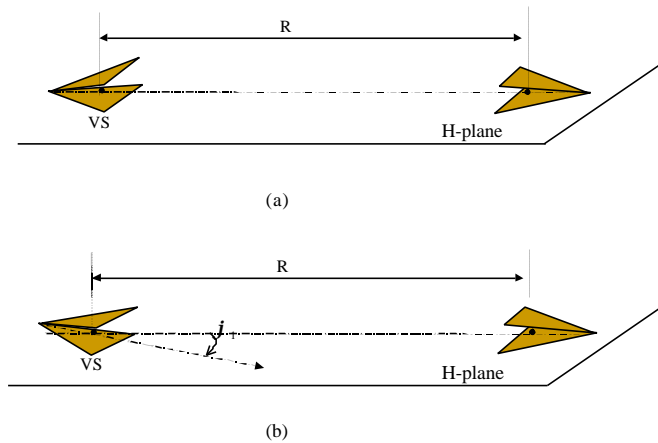


Fig. 4-9: Configuration for the experimental study of the normalised IR off-boresight

The received signal in configuration (a) with two identical antennas on boresight and a distance R between the two virtual sources is given according to (4.17) by

$$V_{rec}(0,0,t) = \frac{1}{2pRc} h_{N,0}(t) \otimes h_{N,0}(t) \otimes \frac{dVs(t)}{dt} \otimes \mathbf{d}(t - t_{d,TX} - t_{d,RX}) \quad (4.21)$$

where $h_{N,0}(t)$ is the normalised IR on boresight.

If the transmitting antenna is rotated in the H-plane by an angle \mathbf{j}_1 around its virtual source, while the receiving antenna is fixed (Fig. 4-9 (b)), the received voltage is given by

$$V_{rec}(0, \mathbf{j}_1, t) = \frac{1}{2pRc} h_N(0, \mathbf{j}_1, t) \otimes h_{N,0}(t) \otimes \frac{dV_S(t)}{dt} \otimes \mathbf{d}(t - t_{d, TX} - t_{d, RX}) \quad (4.22)$$

where $h_N(0, \mathbf{j}_1, t)$ is the normalised IR in the direction $(0, \mathbf{j}_1)$.

The measured voltage $V_{rec}(0, \mathbf{j}_1, t)$ differs from $V_{rec}(0, 0, t)$ by a factor $k_h(\mathbf{j}_1)$

$$V_{rec}(0, \mathbf{j}_1, t) = k_h(\mathbf{j}_1) V_{rec}(0, 0, t) \quad (4.23)$$

where $k_h(\mathbf{j}_1)$ is by definition the value of the p-t-p antenna pattern in the H-plane for an angle \mathbf{j}_1 .

When substituting (4.21) and (4.22) in (4.23) and simplifying the expression, the normalised IR in the direction $(0, \mathbf{j}_1)$ can then be expressed as

$$h_N(0, \mathbf{j}_1, t) = k_h(\mathbf{j}_1) h_{N,0}(t) \quad (4.24)$$

Although the above result is only for a rotation of the antenna in the H-plane, the same result holds for any direction (\mathbf{q}, \mathbf{j}) , hence

$$h_N(\mathbf{q}, \mathbf{j}, t) = k_e(\mathbf{q}) k_h(\mathbf{j}) h_{N,0}(t) \quad (4.25)$$

with $k_e(\mathbf{q})$ and $k_h(\mathbf{j})$ the p-t-p pattern in the E- and the H-plane.

The result in expression (4.25) is very important. It means that an antenna is totally characterised in the time domain if its normalised IR on boresight and its p-t-p pattern in E- and H-plane is known, as far as we stay within the 3dB beamwidth of the antenna.

4.4.4. Relation between gain and normalised IR

The normalised IR totally describes the behaviour of the antennas. This means that it must be possible to derive classical antenna parameters from this normalised IR. As an example we express in this section the gain in terms of the normalised IR [9].

We start with the same expression (4.13) and (4.11) in the frequency domain:

$$P_r(\mathbf{w}) = A_e(\mathbf{w})S_{inc}(\mathbf{w}) \quad (4.26)$$

and

$$G_t(\mathbf{w}) = \frac{4\mathbf{p}}{I^2} A_e(\mathbf{w}) \quad (4.27)$$

where G_t is the antenna power gain, A_e the antenna effective area and S_{inc} the incoming power density. Replacing the effective area in (4.26) by (4.27), we can write

$$P_r(\mathbf{w}) = \frac{I^2}{4\mathbf{p}} G_t(\mathbf{w})S_{inc}(\mathbf{w}) \quad (4.28)$$

Taking the square root of equation (4.28) and recasting to voltages results in

$$\frac{|V_{rec}(\mathbf{w})|}{\sqrt{Z_c}} = \frac{I}{2\sqrt{p}} \sqrt{G_t(\mathbf{w})} \frac{|E_{inc}(\mathbf{w})|}{\sqrt{Z_0}} \quad (4.29)$$

Note that, just like in Chapter 3, the losses due to the reflection coefficients of the antenna feed are included in the gain.

If we convert equation (4.15) to the frequency domain and compare it with equation (4.29) we find the relation between the gain and the normalised IR of the antenna:

$$G_t(\mathbf{w}) = \frac{4p}{I^2} |H_N(\mathbf{w})|^2 \quad (4.30)$$

where $H_N(\mathbf{w})$ is the Fourier transform of the normalised IR (also given by (4.19)).

4.5. Results on TEM horns

The normalised IR describes the antenna performances in a very compact way. In this section the performances on boresight of four different TEM horns are compared. For simplicity the antennas are numbered from 1 to 4. Table 4.1 summarises the physical characteristics of the tested antennas. (L is the length of the antenna plates and A_{ap} the area of the physical antenna aperture). More details on the antennas can be found in Chapter 3.

	L (cm)	A_{ap} (cm ²)	Filling	RAM
Antenna 1	10	10*4	air	no
Antenna 2	10	10*4	dielectric	no
Antenna 3	12	12*6	dielectric	no
Antenna 4	12	12*6	dielectric	yes

Table 4.1: The physical characteristics of the tested antennas

Antenna 4 is the same as antenna 3 but with RAM placed at the outside end of the antenna plates, to reduce the antenna ringing and to suppress the pre-pulse (see Chapter 3, Section 3.5.3). For each antenna, S_{21} was measured between 40 MHz and 20 GHz, with a frequency step of 40 MHz, by placing two identical antennas on boresight. The normalised IRs on boresight of the antennas are shown in Fig. 4-10. Note that the dimensions of $h_N(t)$ are given in m/ns, which corresponds to the dimensions needed in (4.14) and (4.15).

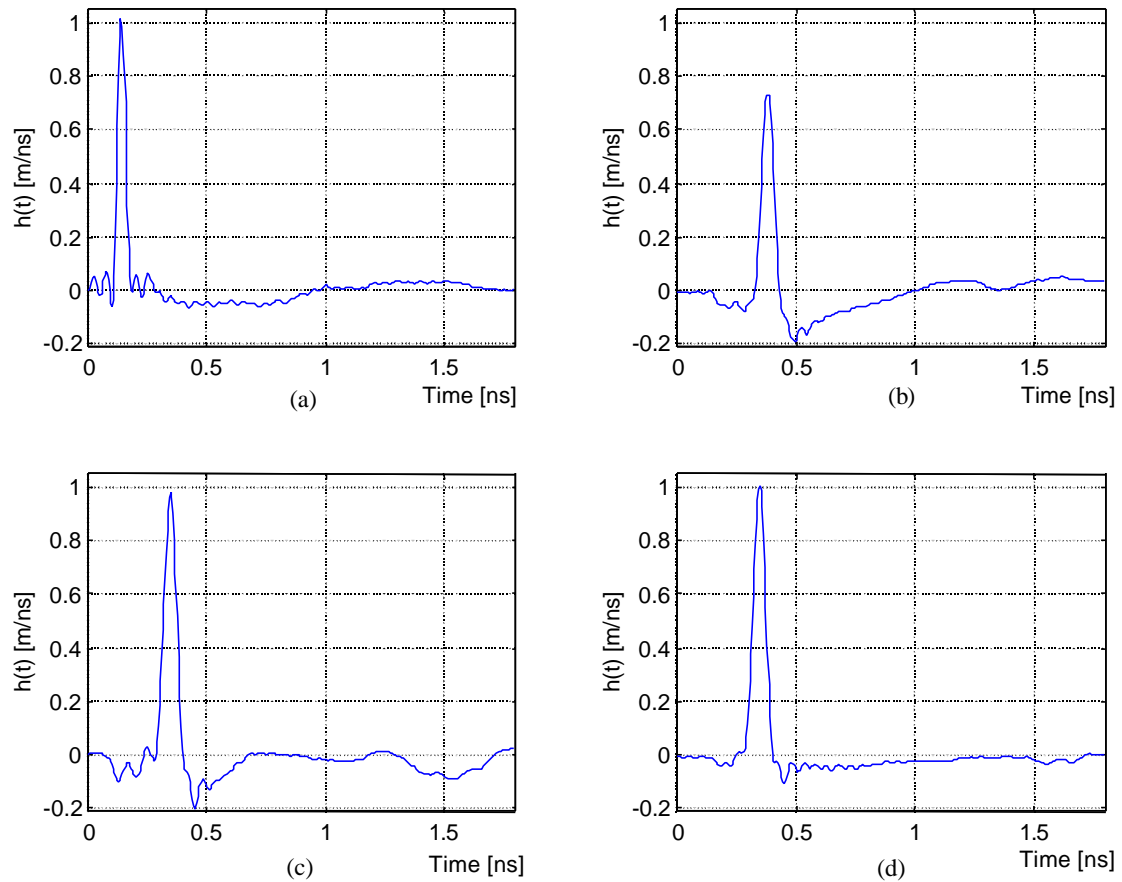


Fig. 4-10: (a) $h_N(t)$ of antenna 1 (b) $h_N(t)$ of antenna 2
(c) $h_N(t)$ of antenna 3 (d) $h_N(t)$ of antenna 4

For a detailed comparison of the antennas, we summarise some important characteristics of the normalised IR in Table 4.2, *i.e.* the maximum value of the normalised IR, the full width at half maximum value (FWHM) of the impulse, the area under the impulse, and the tail fluctuation as a portion of the maximum value.

	Max of $h_N(t)$ [m/ns]	FWHM [ps]	Area under impulse [m]	tail fluctuation [% of max]
Antenna 1	1.01	38	0.038	13%
Antenna 2	0.73	56	0.041	33%
Antenna 3	0.98	60	0.059	22%
Antenna 4	1.01	60	0.062	11%

Table 4.2: Important characteristics of the normalised IR

The FWHM value of the normalised IR is related to the bandwidth of the antenna. The area under the impulse is related to the effective antenna height [4]. It can be seen that filling the antenna with the dielectric reduces the bandwidth, but increases the area under the impulse. The presence of the absorber material at the end of the antenna plates of antenna 4 has a positive influence on the antenna performance. The comparison with antenna 3 shows that the absorber material does not affect the bandwidth nor the area under the impulse, but it considerably decreases the fluctuations in the tail of the response. Thus antenna 4 will be capable of radiating transient pulses with less ringing. It would be difficult to demonstrate this antenna property with the classical frequency domain characterisation of an antenna. In the implementation of a laboratory UWB GPR, which will be described in Chapter 6, antenna 4 is used.

Fig. 4-11 shows the gain of each antenna derived from the normalised IR (the gain is calculated using expression (4.30)). The gain of the dielectric filled TEM horn (antenna 3 and 4) is 10 dB. The results for antenna 1 and antenna 2 are comparable with the frequency domain measurements of the gain shown in Fig. 3-23 of Chapter 3. The lower cut-off frequency of antenna 4 is about the same as the lower cut-off frequency of antenna 2. This means that the prolongation of the antenna plates with 2 cm does not have much influence.

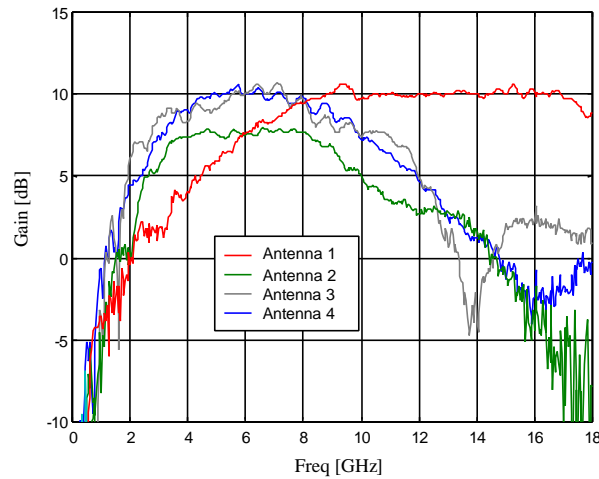


Fig. 4-11: Antenna gain of dielectric filled TEM horn

4.6. Time domain simulations

The normalised impulse response is a powerful tool that also can be used for simulation and system design purposes. Some examples are presented in this section. For each example the simulated data are compared with measured data. The antenna used in the simulations is antenna 4.

Two antennas on boresight

The first simulation is straightforward. Two antennas are put on boresight at a distance of $R = 90$ cm. A very short transient impulse with a maximum amplitude of 2.5 V in a 50Ω load and a FWHM of 90 ps is used as a driving voltage V_s (Fig. 4-12 (a)).

The transient voltage signal V_{rec} at the output of the receiving antenna is calculated using (4.17) and measured using a digitising oscilloscope. Fig. 4-12 (b) shows the calculated waveform and the measured waveform. Both time and voltage data of the two waveforms correspond well.

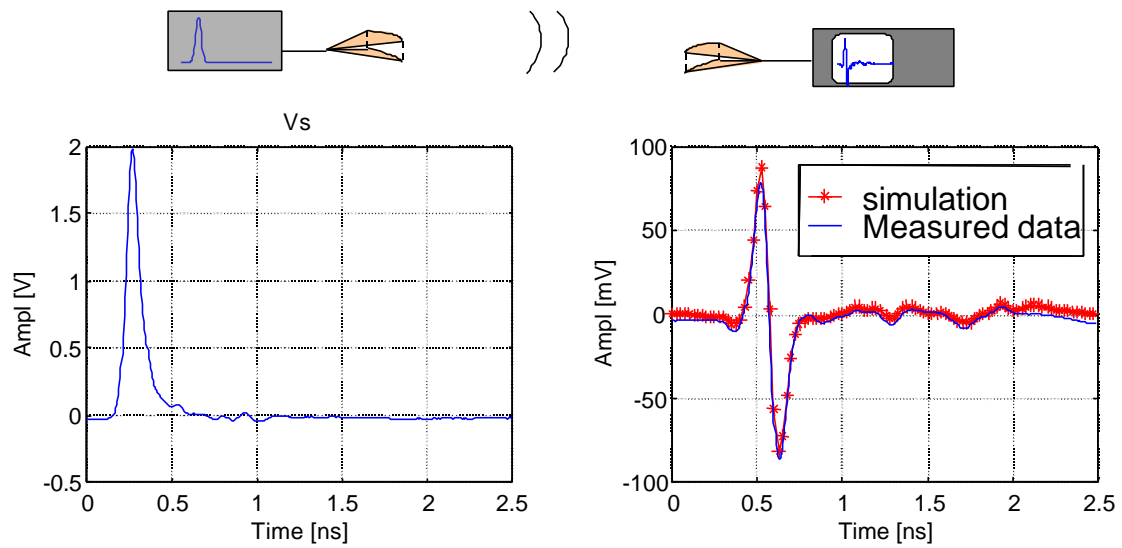


Fig. 4-12: (a) Driving signal V_s

(b) Two antennas on boresight, simulated and measured data

Reflection on a planar air-ground interface

In a second example the reflection on a planar dry sand interface is simulated. The bistatic configuration, typical for ground penetrating radar, is represented in Fig. 4-13. The two antennas are focused at a point on the interface. The distance between the virtual sources of the TEM horns is 22.8 cm. The H-planes of the antennas are in the same plane and the E-field of both antennas is parallel to the interface (normal to the plane of incidence). The driving voltage V_s is the same as in the previous simulation.

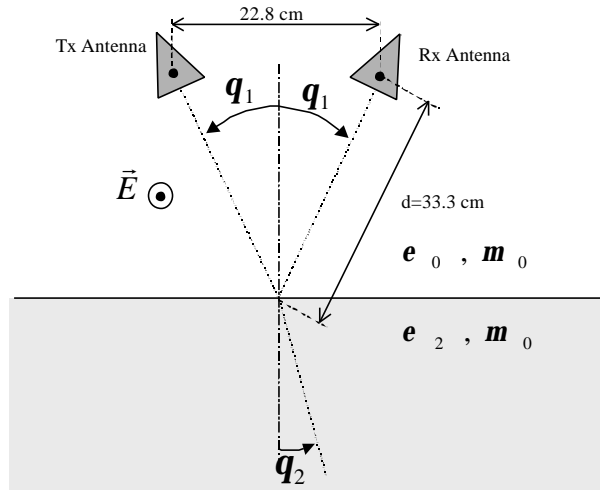


Fig. 4-13: Bistatic configuration

The dry sand is characterised by an \mathbf{e}_r of 2.55 and a \mathbf{m}_r of 1 in the frequency band of interest, and is assumed to be homogeneous and loss-less. The reflection coefficient for a polarisation normal to the plane of incidence, is given by

$$\Gamma_{\perp} = \frac{\sqrt{\mathbf{e}_0} \cos q_1 - \sqrt{\mathbf{e}_2} \cos q_2}{\sqrt{\mathbf{e}_0} \cos q_1 + \sqrt{\mathbf{e}_2} \cos q_2}, \text{ which is } -0.248 \text{ in this case.}$$

The total path loss in the simulation is due to the free-space loss over a distance $2d$ and to the reflection loss from the air-sand interface. The simulated data is obtained by multiplying the result of (4.17) by Γ_{\perp} . Despite the fact that the air-sand interface is near the antennas, the result of the simulation is very similar to the measured data (Fig. 4-14). Note that the direct coupling between transmitting and receiving antennas, which is not taken into account in the simulation, will also introduce errors.

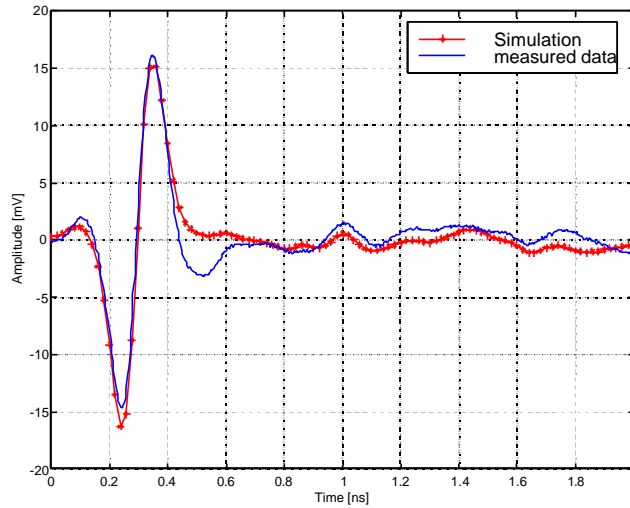


Fig. 4-14: Reflection on a planar dry sand interface, simulated and measured data

Echo of a metallic disc

In the last simulation, the normalised antenna equations are used in combination with commercial FDTD software. The bistatic antenna configuration, almost the same as in the previous example, is represented in Fig. 4-15. An aluminium disc with a radius of 3.2 cm and 1 cm thick is placed at the focus point of the two antennas.

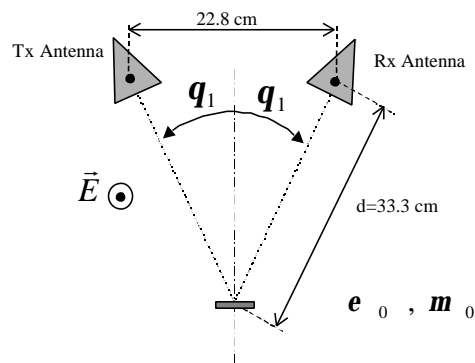


Fig. 4-15: Bistatic configuration for metallic disc

Expression (4.14) is used to calculate the radiated E-field at the metallic disc. This wave, assumed to be planar, is introduced in a FDTD programme, which calculates the backscattered field at a point corresponding to the virtual source of the receiving antenna. Using this backscattered field as an incoming field for expression (4.15), we

calculate the received voltage at the output of the receiving antenna. The simulated data and the measured data are given in Fig. 4-16. Again, the correspondence is good. An advantage of this simulation scheme is that we do not need to model the antennas in the FDTD programme.

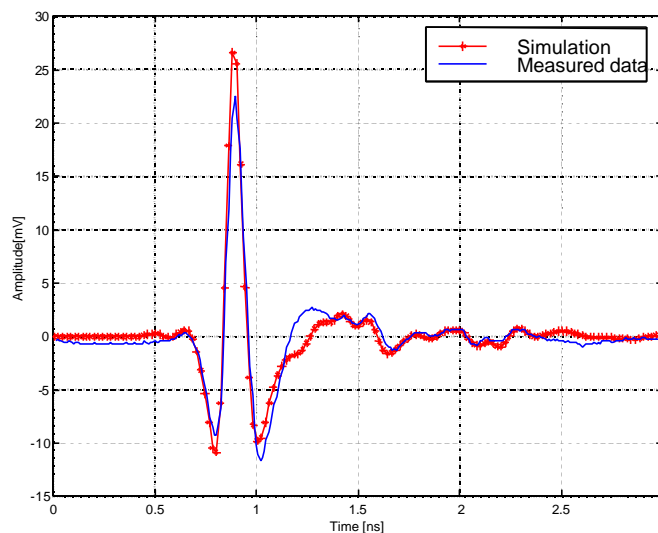


Fig. 4-16: Echo of a metallic disc, simulated and measured data

4.7. Summary

The normalised IR describes time domain antenna performances, which are sometimes difficult to see in classical antenna parameters, in a compact way. The advantage of using the normalised IR over any other impulse response is that all frequency dependent characteristics are included in the normalised IR. This has two important consequences. First, the time domain antenna equations become very simple and accurate to use, without any assumptions about antenna impedance. Second, the normalised IR permits a comparison between different variants of time domain antennas, taking into account all these frequency dependent terms.

We showed that the normalised IR on boresight is easy to measure, using two identical antennas and a vector network analyser. Furthermore, we showed in an experimental study that the normalised IR off-boresight can be derived from the normalised IR on boresight, using the p-t-p antenna pattern. This means that an

antenna is totally characterised in the time domain by its normalised IR on boresight and its p-t-p pattern. Due to the finite but non-zero size of the antenna, the distance from an observation point to the antenna becomes ambiguous for points close to the antenna. The introduction of an apparent point in the antenna, called the virtual source - which can be seen as the origin of the radiated impulse TEM wave - resolves this shortcoming. The position of the virtual source in the antenna can be easily located.

Thanks to the introduction of the virtual source, the antenna equations can now be used near the antenna, as shown in the examples of the time domain simulations. The simulations also demonstrate the simplicity and accuracy of the time domain antenna equations, using the normalised IR. Similar simulations can also be applied for simulating system performance with different transient impulse generators or for radar range estimation. This will be the subject of Chapter 5.

REFERENCES

- [1] E. G. Farr and C. E. Baum, "Extending the Definitions of antenna gain and Radiation Pattern into the Time Domain," *Sensor and Simulation Notes*, note 350, 1992.
- [2] B. Scheers, M. Acheroy, A. Vander Vorst, "Time domain simulation and characterisation of TEM Horns using normalised impulse response," *IEE Proceedings - Microwaves, Antennas and Propagation*, vol. 147, no. 6, pp. 463-468, Dec. 2000.
- [3] P. R. Foster, *Introduction to Ultra-Wideband Radar Systems*. J. D. Taylor, Ed., USA: CRC Press, 1995, ch. 5.
- [4] E. G. Farr and C. E. Baum, "Time Domain Characterization of Antennas with TEM Feeds," *Sensor and Simulation Notes*, note 426, 1998.
- [5] C. E. Baum, "General Properties of Antennas," *Sensor and Simulation Notes*, note 330, 1991.
- [6] R. W. P. King, *Theory of linear antennas*. Cambridge, MA: Harvard University Press, 1956.
- [7] M. Kanda, "Transients in a Resistively Loaded Linear Antenna Compared with those in a Conical Antenna and a TEM Horn," *IEEE Trans. on Antennas Propagat.*, vol. AP-28, no. 1, pp. 132-136, 1980.
- [8] A. V. Oppenheim and R. W. Schaffer, *Digital Signal Processing*. New Jersey: Prentice-Hall, 1975.
- [9] L. H. Bowen, E. G. Farr and W. D. Prather, "Fabrication of two collapsible Impulse Radiating Antennas," *Sensor and Simulation Notes*, note 440, 1999.